NASA TECHNICAL NOTE

NASA TN D-7459

NASA TN D-7459

DESCRIPTION AND SIMULATION OF AN INTEGRATED POWER AND ATTITUDE CONTROL SYSTEM CONCEPT FOR SPACE-VEHICLE APPLICATION

by Ralph W. Will, Claude R. Keckler, and Kenneth L. Jacobs

Langley Research Center
Hampton, Va. 23665

NATIONAL AERONAUTICS AND SPACE ADMINISTRATION • WASHINGTON, D. C. • APRIL 1974

1. Report No.	2. Government Accession No.	3. Recipient's Catalog No.
NASA TN D-7459		

4. Title and Subtitle	5. Report Date
DESCRIPTION AND SIMULATION OF AN INTEGRATED POWER AND ATTITUDE CONTROL SYSTEM CONCEPT FOR SPACE-VEHICLE APPLICATION	April 1974
	6. Performing Organization Code
7. Author(s)	8. Performing Organization Report No.
Ralph W. Will, Claude R. Keckler, and Kenneth L. Jacobs	L-8791
	10. Work Unit No.
9. Performing Organization Name and Address	909-74-35-01
NASA Langley Research Center Hampton, Va. 23665	11. Contract or Grant No.
	13. Type of Report and Period Covered
12. Sponsoring Agency Name and Address	Technical Note
National Aeronautics and Space Administration Washington, D.C. 20546	14. Sponsoring Agency Code

15. Supplementary Notes

16. Abstract

An Integrated Power and Attitude Control System (IPACS) concept with potential application to a broad class of space missions is discussed. A description is given of the basic concept of combining the onboard energy storage and attitude control functions by storing energy in spinning flywheels which are used to provide control torques. A shuttle-launched Research and Applications Module (RAM) A303B solar-observatory mission having stringent pointing requirements (1.0 arc second) is selected to investigate possible interactions between energy storage and attitude control. A simulation of this spacecraft involving actual laboratory-model control-system hardware is presented. Simulation results are discussed which indicate that the IPACS concept, even in a failure-mode configuration, can readily meet the RAM A303B pointing requirements.

17. Key Words (Suggested by Author(s))	18. Distribution Statement
Attitude control Control moment gyro Research and applications module	Unclassified – Unlimited STAR Category 31

19. Security Classif. (of this report)	20. Security Classif. (of this page)	21. No. of Pages	22. Price*
Unclassified	Unclassified	30	$3.25

*For sale by the National Technical Information Service, Springfield, Virginia 22151

DESCRIPTION AND SIMULATION OF AN INTEGRATED POWER AND ATTITUDE CONTROL SYSTEM CONCEPT FOR SPACE-VEHICLE APPLICATION

By Ralph W. Will, Claude R. Keckler, and Kenneth L. Jacobs
Langley Research Center

SUMMARY

An Integrated Power and Attitude Control System (IPACS) concept with potential application to a broad class of space missions is discussed. A description is given of the basic concept of combining the onboard energy storage and attitude control functions by storing energy in spinning flywheels which are used to provide control torques. A shuttle-launched Research and Applications Module (RAM) A303B solar-observatory mission having stringent pointing requirements (1.0 arc second) is selected to investigate possible interactions between energy storage and attitude control. A simulation of this spacecraft involving actual laboratory-model control system hardware is presented. Simulation results are discussed which indicate that the IPACS concept, even in a failure-mode configuration, can readily meet the RAM A303B pointing requirements.

INTRODUCTION

Momentum storage devices are normally used to provide attitude control torques for missions where reaction control system fuel requirements or environment contamination are excessive. Momentum storage devices provide attitude control torques by either the direct angular acceleration of a spinning flywheel (reaction wheel) or by the precession of spinning flywheel (control moment gyroscope). The technique of direct angular acceleration of the spinning flywheels in a reaction wheel system to produce control torque allows low torque threshold capability but is limited by flywheel speed. As the speed of the flywheel increases, an increase in electrical power is required to produce the same torque level. On the other hand, flywheels of the control-moment-gyroscope (CMG) system are held at high constant speeds and the wheels are rotated normal to their spin vectors (precession). This provides high-level control torque with low total power requirement. If large momentum and torque range with low electrical power are required, the CMG system is an obvious choice. The Skylab CMG system,

discussed in references 1 and 2 and shown in figure 1, is an example of such a system. Three double-gimbal CMG units with constant-speed flywheels, each having 3120 N-m-sec of momentum, are precessed in a controlled manner to maneuver the vehicle to a selected attitude and then to hold that attitude.

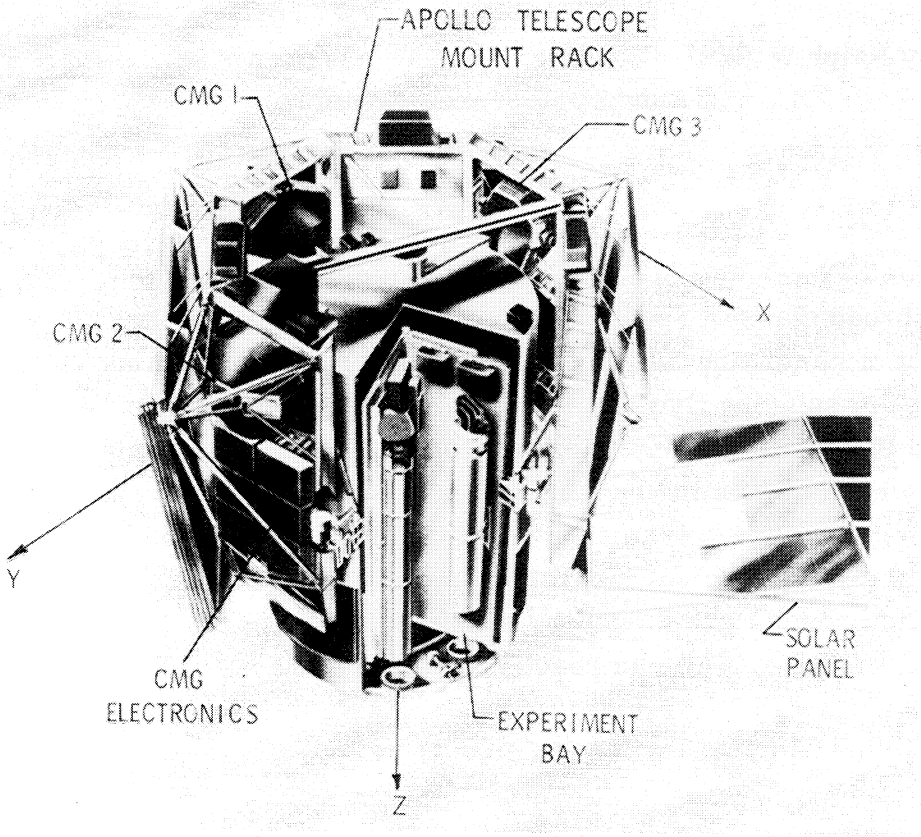

Figure 1.- Double-gimbal CMG configuration for Skylab.

Since there is no requirement to produce control torque by direct acceleration of the flywheels of a CMG system, the spin speeds of the flywheels offer available degrees of freedom. It has been proposed by R. Gorman at Bellcomm, Incorporated, that the CMG flywheels be used for energy storage by adding flywheel motor-generator units; the wheels, thus, replace a large percentage of the spacecraft electrical storage batteries, thereby allowing potentially significant weight and cost savings. This combined system is called an Integrated Power and Attitude Control System (IPACS).

The potential weight savings to be realized from this concept can be seen by noting the energy density capability of various proposed flywheel materials as compared with existing battery technology. In references 3, 4, and 5 test data have shown that current

material technology can be used to develop a low-cost flywheel with an energy density up to four times the energy density of nickel-cadmium batteries currently used in spacecraft.

Adding energy storage capability to a CMG system introduces two new requirements concerning control torque development. These are given as follows: (1) The IPACS units must provide precession torques to null the direct-acceleration torques produced when increasing or decreasing the kinetic energy of the flywheels; and (2), the system must compensate for loss of flywheel momentum when a large energy requirement is placed on the system. Fortunately, the magnitudes of the direct-acceleration torques are small for nominal flywheel speeds, being of the order of 0.4 N-m for the Skylab wheels if a ground rule of 75 percent energy discharge over a half-orbit is chosen. Also, the fact that flywheel energy is proportional to the square of speed, whereas momentum varies directly with speed, allows a large range in stored energy for a moderate range of stored momentum. (For example, a 10-percent change in momentum represents a 21-percent change in energy.)

SYMBOLS

G_X, G_Y, G_Z	negative of CMG system output torques resolved about spacecraft axes, N-m
$G_{X,j}, G_{Y,j}, G_{Z,j}$	individual CMG output torques resolved about spacecraft axes, (where $j = 1,2$), N-m
H	magnitude of individual CMG momentum, N-m-sec
$\overline{H}_1, \overline{H}_2$	CMG momentum vectors
$\overline{H}_T$	total IPACS system momentum vector
H_1, H_2	magnitudes of $\overline{H}_1$ and $\overline{H}_2$, N-m-sec
H_T	magnitude of $\overline{H}_T$, N-m-sec
$\dot{H}$	rate of change of CMG momentum, N-m
$\dot{H}_{X''}, \dot{H}_{Y''}, \dot{H}_{Z''}$	rates of change of system momentum about the X''-, Y''-, and Z''-axes (CMG momentum axes), respectively, N-m
I_X, I_Y, I_Z	spacecraft inertias about X-, Y-, and Z- (principal) axes, respectively, kg-m^2

$K_{X,a}, K_{Y,a}, K_{Z,a}$	CMG system control law attitude gains about spacecraft axes, N-m/rad
$K_{X,r}, K_{Y,r}, K_{Z,r}$	CMG system control law rate gains about spacecraft axes, N-m/rad/sec
$M_{X,c}, M_{Y,c}, M_{Z,c}$	CMG system command moments about spacecraft axes, N-m
S	Laplace operator
$T_{X''}, T_{Y''}, T_{Z''}$	CMG output torques resolved about CMG momentum axes, N-m
t	time, sec
X, Y, Z	spacecraft principal axes
X', Y', Z'	intermediate rotation axes (see fig. 3(b))
X'', Y'', Z''	CMG system momentum axes
α	simulated CMG gimbal angle, deg
$\dot{\alpha}$	simulated CMG gimbal rate, deg/sec
$\dot{\alpha}_c$	CMG command gimbal rate, deg/sec
$\ddot{\alpha}$	simulated CMG gimbal acceleration, deg/sec^2
β	CMG system angle, $\frac{\beta_1 + \beta_2}{2}$ (see fig. 3(b))
β_1, β_2	CMG inner gimbal angles, deg
$\dot{\beta}$	CMG system precession rate (see fig. 3(b))
$\dot{\beta}_1, \dot{\beta}_2$	CMG inner gimbal rates, deg/sec
δ	CMG system scissor angle, $\frac{\lvert\beta_1 - \beta_2\rvert}{2}$, deg (see fig. 3(b))

$\dot{\delta}$	rate of change of CMG system scissor angle, deg/sec
ρ	simulated CMG servo-loop damping ratio
ρ_n	CMG system control-law damping ratio
φ,θ,ψ	spacecraft error angles about X-, Y-, and Z-axes, respectively, arc sec
$\varphi_o,\theta_o,\psi_o$	initial conditions for spacecraft error angles, arc sec
ω	simulated CMG servo-loop natural frequency, rad/sec
ω_n	CMG system control-law natural frequency, rad/sec
ω_W	CMG wheel-speed command, rpm
$\omega_X,\omega_Y,\omega_Z$	spacecraft body rates about the X-, Y-, and Z-axes, respectively, (arc sec)/sec
$\dot{\omega}_X,\dot{\omega}_Y,\dot{\omega}_Z$	spacecraft angular accelerations about the X-, Y-, and Z-axes, respectively, (arc sec)/sec^2

Abbreviations:

A/D	analog to digital
CMG	control moment gyroscope
D/A	digital to analog
IPACS	Integrated Power and Attitude Control System
RAM	Research and Applications Module
RCS	Reaction Control System
TMS	torque measuring system

SYSTEM DESCRIPTION

The major elements of an IPACS are shown in figure 2(a). Solar energy is converted into electrical energy by a solar panel array and then is properly conditioned (voltage, frequency, etc.) either for direct use by the spacecraft subsystems or for conversion to mechanical energy and storage in IPACS units. The IPACS unit sketched in figure 2(a) is a single-rotor double-gimbal device which is a typical component of a complete three-axis attitude control system. Slip rings are used in the unit to transfer energy across the gimbal pivots and to permit complete freedom for gimbal rotation. Gimbal actuator and sensor packages containing torque motors and position and rate sensors are used to precess the flywheel to produce the desired control torques. A tachometer measures spin speed and allows flywheel momentum and energy ("charge") to be computed.

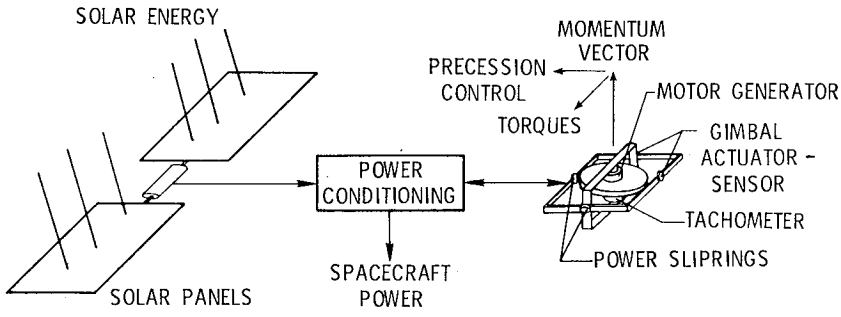

(a) Primary IPACS elements.

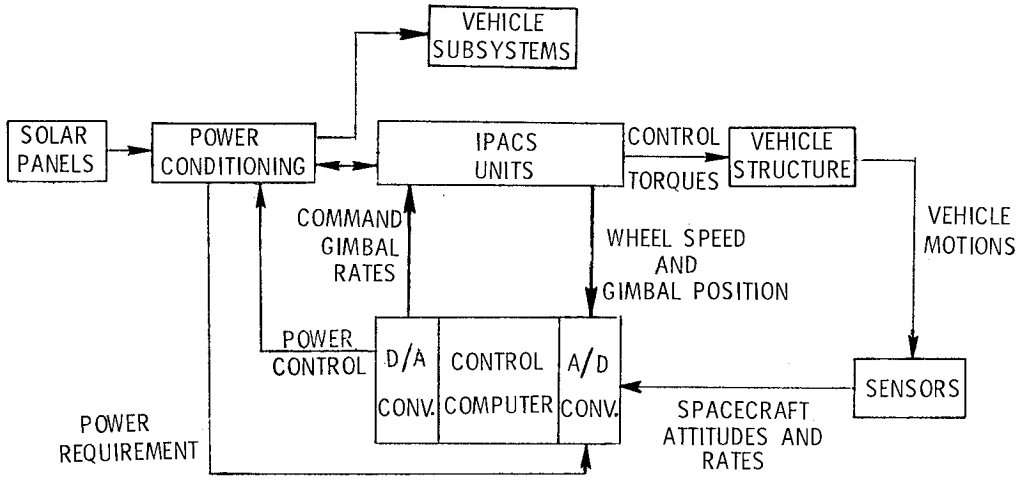

(b) Signal and power flow.

Figure 2.- Schematic diagrams of IPACS.

Signal and power flow are illustrated in figure 2(b). Spacecraft attitudes and attitude rates, IPACS unit flywheel speeds, and gimbal positions are read into a digital control computer through analog-to-digital (A/D) converters. The control computer also obtains information from sensors within the power-conditioning equipment to determine solar panel output and spacecraft power requirements and then routes appropriate power to the IPACS wheels. Spacecraft attitudes and attitude rates are compared with the desired reference and the differences are nulled by commanding appropriate control torques. The control torques are achieved by flywheel precession at rates determined by a steering law. A steering law involves a matrix inversion which relates output torques to precession rates, flywheel speeds, and gimbal availability. Because of the complex and highly nonlinear dynamics of the IPACS units with the inherent limits on stored momentum, extensive control computations and storage are necessary to achieve the desired control torques. This requires the implementation of a digital control computer rather than an analog device.

The CMG configuration described in reference 6 has been selected for implementation as an IPACS application. The complete system consists of two double-rotor, double-gimbal units like the single unit shown in figure 3(a). The configuration considered here represents a "worst case" or failure-mode condition in which one unit would be shut down. Spacecraft control is then provided by a single double-rotor, double-gimbal unit exactly as depicted in figure 3(a).

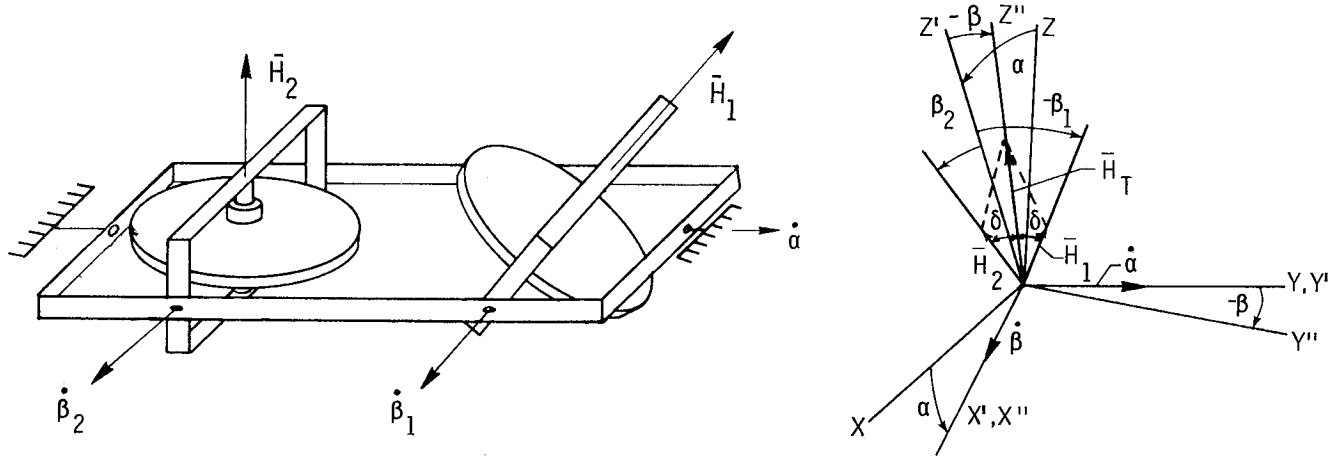

(a) Schematic diagram of IPACS configuration. (b) Coordinate system.

Figure 3.- Double-rotor double-gimbal IPACS configuration.

The steering law for a single unit will be outlined to illustrate the interaction between power and torque requirements. The coordinates used are shown in figure 3(b). Spacecraft power is stored equally in the two wheels so that the magnitudes of their momenta $(H_1$ and $H_2)$ are always equal. The two axis systems involved are the spacecraft (X,Y,Z) axes alined with the spacecraft principal axes and the system momentum (X'',Y'',Z'') axes alined with the total system momentum vector and the inner gimbals of the unit. The two wheels then operate as a scissored pair where torque may be applied directly about the Z''-axis by a change in the system scissor angle δ. The angle δ determines the magnitude of the total system momentum vector. The direction of this vector in spacecraft coordinates is defined by the angles α and β, which are the angles between the X''- and Y''-system momentum axes and the respective X- and Y-spacecraft axes.

From inspection of figure 3(b), the following equation can be written:

$$\begin{Bmatrix} T_{X''} \\ T_{Y''} \\ T_{Z''} \end{Bmatrix} = \begin{bmatrix} \cos\alpha & 0 & -\sin\alpha \\ \sin\alpha\sin\beta & \cos\beta & \cos\alpha\sin\beta \\ \sin\alpha\cos\beta & -\sin\beta & \cos\alpha\cos\beta \end{bmatrix} \begin{Bmatrix} M_{X,c} \\ M_{Y,c} \\ M_{Z,c} \end{Bmatrix} \tag{1}$$

The torques, $T_{X''}$, $T_{Y''}$, and $T_{Z''}$, are developed by precessing the gimbals at rates determined subsequently by noting that the resultant momentum vector $\overline{H}_T$ of the system lies (by definition) along the Z''-axis. The speeds of the two rotors are commanded to be equal so that $H_1 = H_2 = H$. Then, from figure 3(b),

$$\dot{H}_{X''} = H_T\dot{\alpha}\cos\beta \tag{2a}$$

$$\dot{H}_{Y''} = -H_T\dot{\beta} \tag{2b}$$

$$\dot{H}_{Z''} = 2(\dot{H}\cos\delta - H\dot{\delta}\sin\delta) \tag{2c}$$

From equation (2c), it can be seen that flywheel energy changes $\dot{H}$ may be compensated for by precession of the two flywheels $\dot{\delta}$, and, thus, energy-momentum coupling can be handled in a simple fashion. Since changes of momentum are the negatives of required control torques, the required precessional rates are determined directly from equations (2) as

$$\left.\begin{aligned} \dot{\alpha} &= \frac{-T_{X''}}{H_T \cos \beta} \\ \dot{\beta} &= \frac{T_{Y''}}{H_T} \\ \dot{\delta} &= \frac{\frac{-T_{Z''}}{2} + \dot{H} \cos \delta}{H \sin \delta} \end{aligned}\right\} \tag{3}$$

Then, by defining

$$\left.\begin{aligned} \beta &= \frac{\beta_1 + \beta_2}{2} \\ \delta &= \frac{\left|\beta_1 - \beta_2\right|}{2} \end{aligned}\right\} \tag{4}$$

the individual CMG gimbal rates become

$$\left.\begin{aligned} \dot{\beta}_{1,c} &= \dot{\beta} + \dot{\delta} \\ \dot{\beta}_{2,c} &= \dot{\beta} - \dot{\delta} \end{aligned}\right\} \tag{5}$$

where the subscript c denotes command values.

EXAMPLE MISSION CHARACTERISTICS

A major concern with the IPACS concept involves the possibility of adverse control interactions produced by torques generated during power-transfer operations. A candidate mission with stringent pointing, stability, and relatively large energy-storage requirements has, therefore, been selected in order to investigate these effects. The spacecraft chosen for study is representative of a class of low earth-orbit spacecraft which have been designated as shuttle-launched Research and Applications Modules (RAM). The particular mission considered is an advanced solar observatory, RAM A303B, shown in figure 4. The RAM spacecraft and mission requirements are described in reference 7. A computer simulation of a growth version of the RAM free-flyer with A303B pointing requirements has been performed.

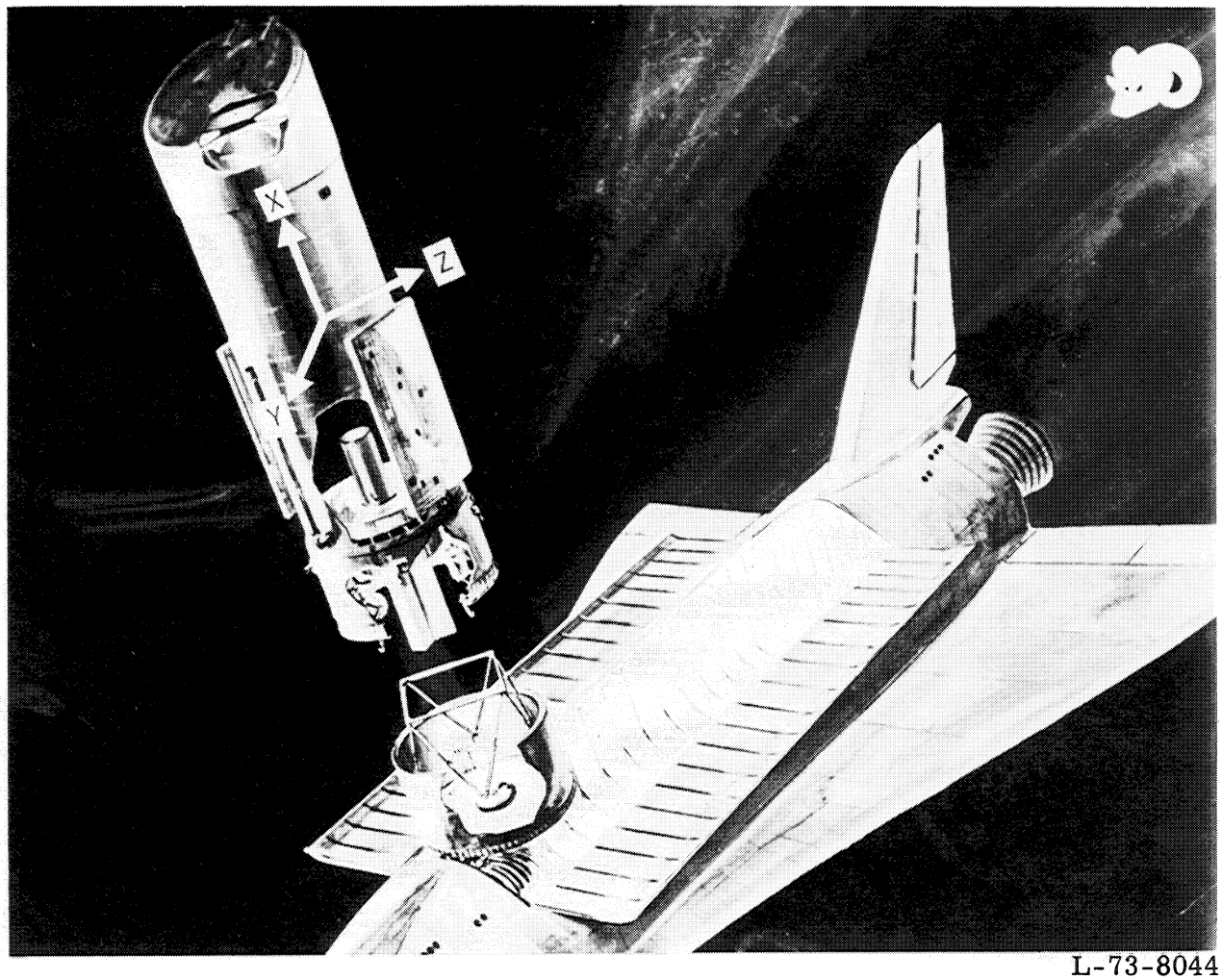

L-73-8044

Figure 4.- Mission selected for simulation.

An IPACS system for attitude control and energy storage has been configured for this vehicle. This report is concerned with this application. The attitude control requirements for this mission are 1.0-arc-second pointing accuracy with 0.02-arc-second pointing stability about the spacecraft Y- and Z-axes during an observation. Observation periods are to be less than 45 minutes in length (approximately one-half the period of the recommended 560-km orbit). The third spacecraft axis is to be stabilized to 0.25^{o}. Minimum momentum-storage requirements for the spacecraft from gravity gradient and aerodynamic torque and from slewing requirements are estimated in reference 7, page IX-12, to be 2034 N-m-sec. Although the spacecraft would not be manned (except for a revisit for servicing) and crew-motion disturbances would not be present, the level of required pointing stability is stringent.

The spacecraft disturbances come from two sources: the experiment package itself and the external environment. Environmental torques include gravity-gradient effects

which are sinusoidal at twice the orbital frequency with a maximum amplitude of 0.637 N-m and aerodynamic disturbances with a maximum amplitude of 0.678 N-m and a frequency equal to the orbital frequency. Experiment-induced disturbances, typified by the operation of protective doors in the Skylab data on page IX-17 of reference 7, should not normally occur during experiment periods, but they have been included to show effects of short-term disturbances.

As previously mentioned, the IPACS configuration selected consists of a single double-rotor double-gimbal unit exactly as shown in figure 3(a). This represents a failure mode for the system of reference 6, since failure of one wheel would necessitate shutting down one of the two units. Under failure conditions, this configuration is required by mission ground rules to provide 85 percent of nominal energy storage capability or 2.2 kW-hr. The CMG rotors are sized primarily from energy considerations. The momentum level is maintained at a minimum consistent with mission requirements by operating at high rotor speeds. This results in a weight and volume effective system design.

Rockwell International, under contract NAS1-11732, has developed a wheel design which operates at a maximum speed of 45 000 rpm and provides 1.1 kW-hr of energy over a speed-reduction range of 50 percent. The wheels operating at half-speed provide a momentum level of 1112 N-m-sec per wheel, which is slightly greater than the 2034 N-m-sec total system requirement. The CMG gimbal torquers are sized for a maximum output of 14.02 N-m as required by the maximum gimbal rates given in reference 7, page IX-16.

Although mission ground rules dictate reverting to reaction-control-system (RCS) operation for this type of failure, undesirable contamination effects would result from this measure. This simulation investigates the capability of IPACS carrying out the stringent pointing tasks under these conditions and is felt to represent a "worst case" for IPACS application.

SIMULATION DESCRIPTION

The spacecraft equations of motion and control algorithms are programed on an EAI 690 hybrid computing system. This system includes an EAI 640 digital computer which is used to simulate the spacecraft control computer. The machine is a good representation of a typical spacecraft flight computer in terms of speed and word size.

Figure 5 shows a simplified block diagram of the IPACS hybrid simulation program and indicates how each system element is represented on the computer. The spacecraft and control system dynamics and the system control law are simulated on the analog portion of the computer. The CMG steering law is programed on the digital computer which represents the spacecraft onboard computer. Appendix A contains a complete set

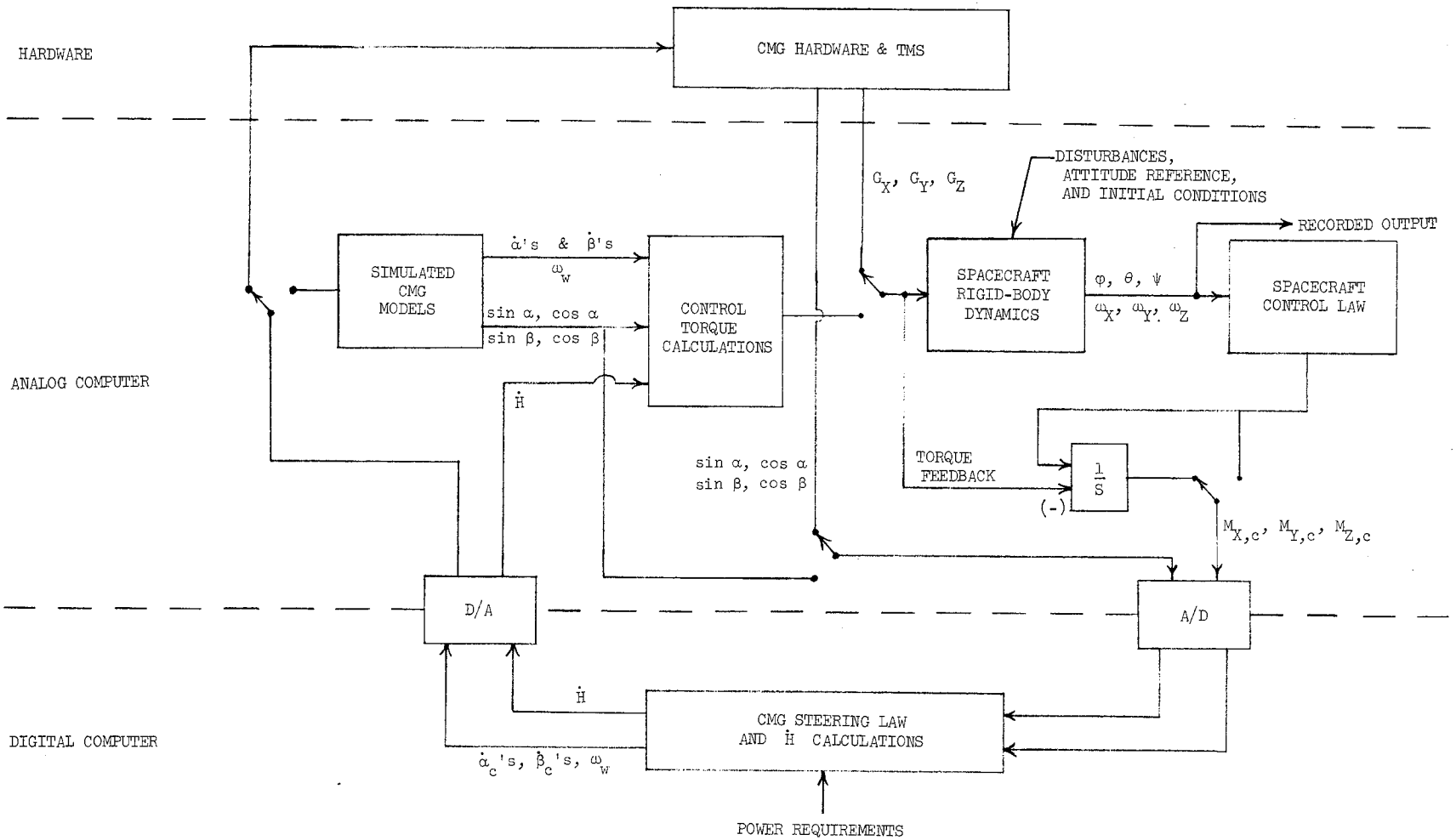

Figure 5.- Functional block diagram of IPACS simulation.

of the equations used for each element of figure 5, whereas appendix B contains a FORTRAN listing of the digital computer routine.

The CMG hardware is mounted on a three-axis torque measuring system (TMS) which is linked to the analog portion of the EAI 690 system through signal transmission lines. A program option permits either the CMG hardware or the CMG models simulated on the analog computer to be used in the control loop. The spacecraft rigid body is initialized relative to the attitude reference, and the resulting error angles generate command moments via the spacecraft control law. These command moments, along with the gimbal-angle sine and cosine functions from either the hardware or simulated CMG units, are transmitted to the digital computer through 12-bit analog-to-digital (A/D) conversion equipment. Spacecraft power requirements which produce momentum changes $\dot{H}$ are also used by the digital computer.

The digital calculations are carried out by using a 23-bit mantissa and the output gimbal-rate commands are routed through 12-bit digital-to-analog (D/A) converters. The digital computer is timed to operate at 10 iterations per second, and the computation cycle requires approximately 90 milliseconds. This means that there is a 90-millisecond delay between the sampling of the command moments and the issuing of gimbal-rate commands based on this information. At 10 iterations per second, this leaves approximately 10 milliseconds before the next sample is taken.

The digital computer output gimbal-rate and wheel-speed commands are transmitted to either the CMG hardware or the simulated CMG models. In addition, the change in wheel momentum $\dot{H}$ is routed to the torque calculations associated with the simulated CMG units to be converted into spacecraft body coordinates, is added to the control torques, and is then applied to the spacecraft. In the hardware case, the wheel-speed commands actually accelerate or decelerate the CMG rotors, and the resulting torques are measured by the TMS along with the control torques.

The CMG system output torques are applied to the spacecraft rigid body and the resulting motions are recorded. The output torques are also used in a torque feedback loop which uses the difference between the commanded torque from the control law and the torque actually being applied to the spacecraft. This difference is then integrated and used in place of the spacecraft control-law command moments M_c as a program option. This feedback is utilized to increase system response and smooth steady-state noise characteristics.

The IPACS control loop is a sampled data system at 10 iterations per second and with an accuracy limited primarily by the analog-digital interface. The simulation using model CMG hardware is a realistic representation of an IPACS system with a digital

onboard computer. Only spacecraft sensor noise and sensor dynamics are not included. Simulation scaling for each system element is given in appendix A with the appropriate equations.

HARDWARE DESCRIPTION

The hardware utilized in the IPACS simulation consists of two double-gimbaled model CMG units (fig. 6) with a maximum momentum capacity of 1.78 N-m-sec per

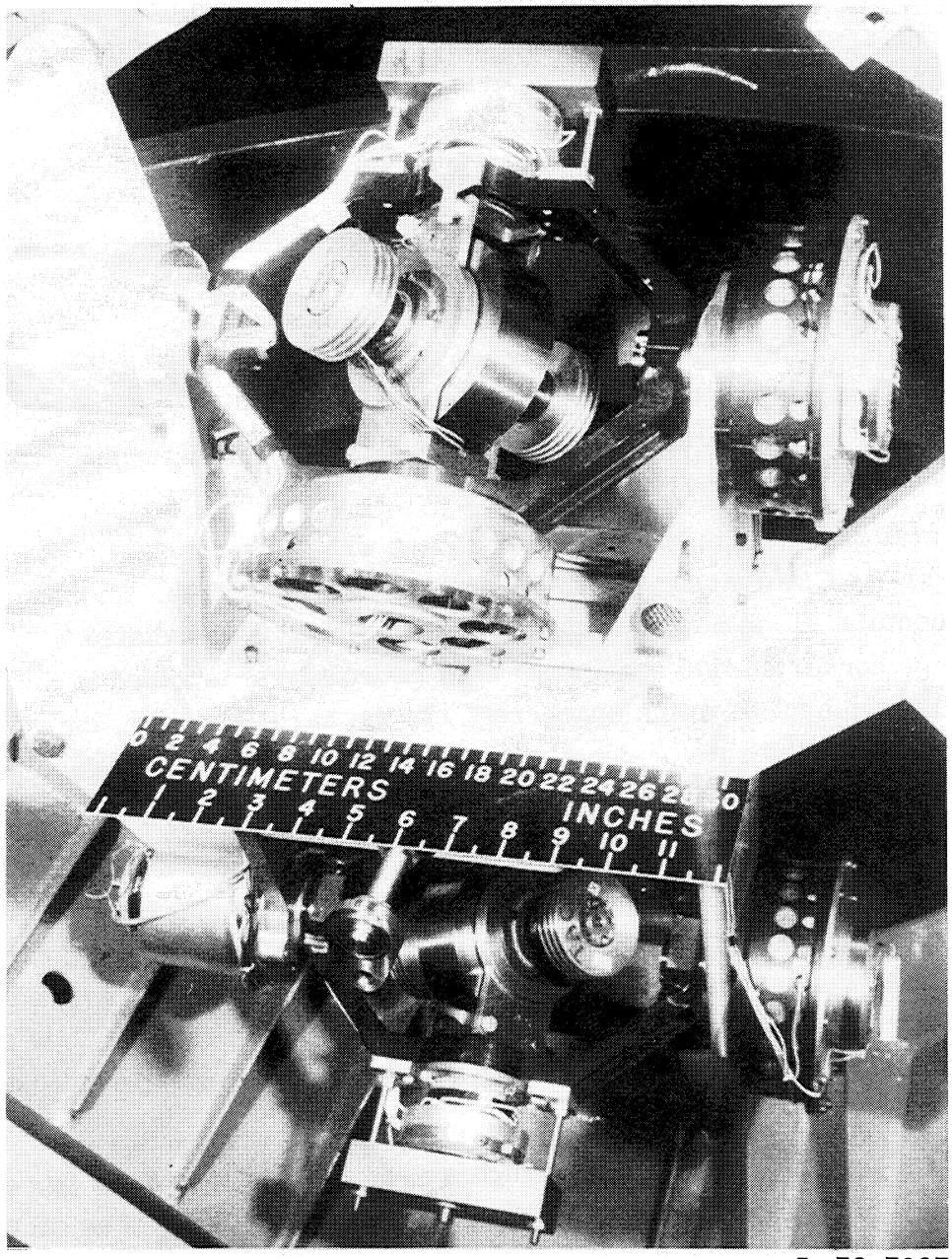

L-72-7907

Figure 6.- Hardware units for IPACS scaled model.

gyroscope. These units are statically mounted on the inner cradle of a three-axis torque measuring system (TMS) which measures the output torques of the CMG units. This information is then transmitted to the computer simulation and is used as control system input to the spacecraft dynamics.

The CMG units are driven by direct-drive dc torquers; thus, potential problems associated with gear trains are eliminated. Each gimbal is equipped with a tachometer to close the rate servo loop and with a sine-cosine resolver for gimbal position information.

Electronic control circuits have been designed to operate the CMG rotor at the appropriate speed as well as to accept commands from the hybrid computer either to accelerate or decelerate the rotor. The computer actually commands wheel speed directly and the control circuits match the command. These speed variations are used to represent the power storage or generation functions of IPACS.

The torque measuring system is a three-axis measuring device which utilizes strain-gage balances to determine the torque output of the internally mounted payload, in this case the CMG units. Side and axial loads, as well as bending moments, are eliminated by the use of isolation flexures.

The TMS has a torque capacity ranging from 0.0054 N-m up to 371.2 N-m. The low torque level and the resolution are limited by the noise produced by the electronics. The lowest natural frequency of the measuring system is in excess of 10 hertz which is well above the overall spacecraft-system frequency and, thus, is not a limiting factor to the simulation.

The two model CMG units are mounted on the inner cradle of the TMS and are operated as a double-rotor, double-gimbal unit. This operation is accomplished by simultaneously controlling the two outer gimbals through a nulling circuit programed on the digital computer (appendix B), thus simulating the single outer gimbal mounting of the two rotors.

DISCUSSION OF RESULTS

The IPACS simulation was developed and the control loop checked out by using the simulated CMG models. However, hardware results will be discussed first. The simulated system data are presented to indicate the performance of perfect hardware. The IPACS test program was set up to include hardware in order to demonstrate the system operation under hardware noise, bandwidth, and nonlinearity constraints. The results achieved in their presence are much more indicative of IPACS concept performance in an actual system application than are pure simulated system results. The

stringent pointing accuracies (1.0 arc second) associated with the selected mission raise questions concerning the performance of IPACS under realistic hardware effects. A control-actuator hardware demonstration of the pointing for the RAM A303B mission, given perfect spacecraft sensors, was, therefore, one of the objectives of the test program.

The hardware test equipment provides a momentum scale factor of approximately 1:1250 compared with the spacecraft system. This leads to problems with the torque measuring system (TMS) since the maximum system torques of 14.92 N-m scaled to less than 0.01356 N-m. The TMS has a design threshold of 0.0054 N-m and exhibits a measured noise level of ± 0.0014 N-m so that most of the system control torques could not be detected. The CMG gimbal rates were, therefore, increased by a factor of 10 so that the overall torque scaling was reduced to approximately 1:125. This measure improved the simulation performance appreciably.

The simulation runs are configured to show several types of control system response and steady-state effects. A basic sequence of events was followed for all simulation runs. The spacecraft was initially offset about all three axes to illustrate the acquisition and settling times of the spacecraft control law while simultaneously counteracting the effects of external disturbances and wheel-speed variations $\dot{H}$ resulting from energy transfer. The external disturbance torques caused the spacecraft motions to settle about constant offset error angles. These external bias torques were then removed to show basic system response to step changes in torque and to allow the recorder traces to be scaled up to illustrate the system and hardware noise-induced motions. Since the high recorder scale setting showed small spacecraft motions, the wheel-speed changes $\dot{H}$ were removed and then reapplied to indicate system response to energy transfer demands. The experiment-induced disturbances were subsequently applied to the spacecraft to illustrate transient effects resulting from a high-level, short-period disturbance torque. Finally, the effectiveness of the torque feedback loop in compensating for hardware noise and nonlinearities were demonstrated by deleting it from the control loop.

The computed IPACS response to initial spacecraft offset errors is shown in figure 7 for offsets of 25, 2.5, and 2.5 arc seconds about the X', Y', and Z'-spacecraft axes, respectively. Initially, both CMG outer gimbal angles are 45° with $\beta_1 = 30^{\circ}$ and $\beta_2 = -30^{\circ}$.

Figure 7(a) represents the IPACS with full momentum (H = 2224 N-m-sec), and figure 7(b) represents an identical run with half-momentum (H = 1112 N-m-sec). The spacecraft motions are similar; thus, it is shown that there is little effect on system response caused by the varying momentum storage of IPACS.

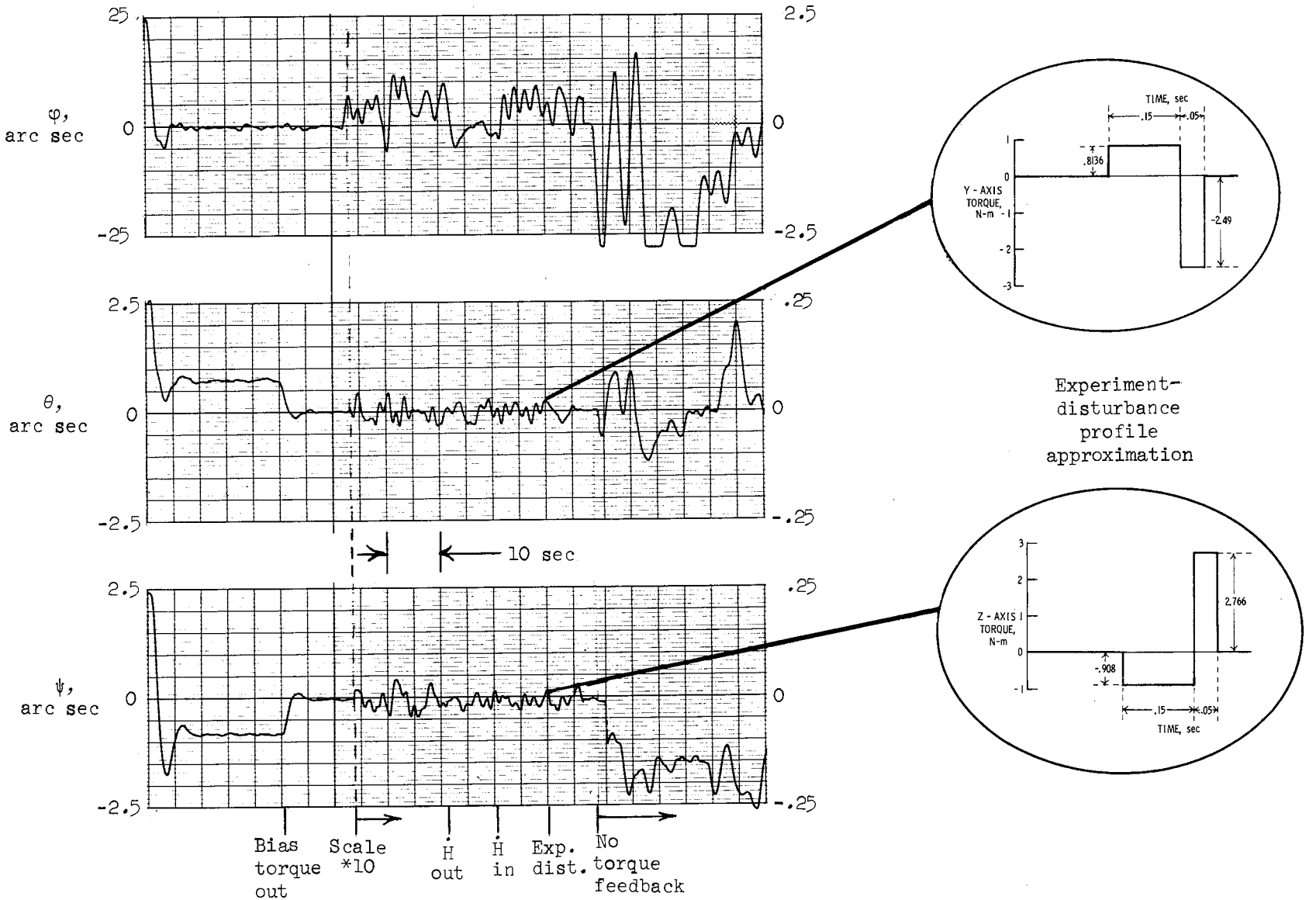

(a) Full H; $\dot{H}$ = -0.2712 N-m per wheel.

Figure 7.- Computed IPACS response with scaled model hardware.

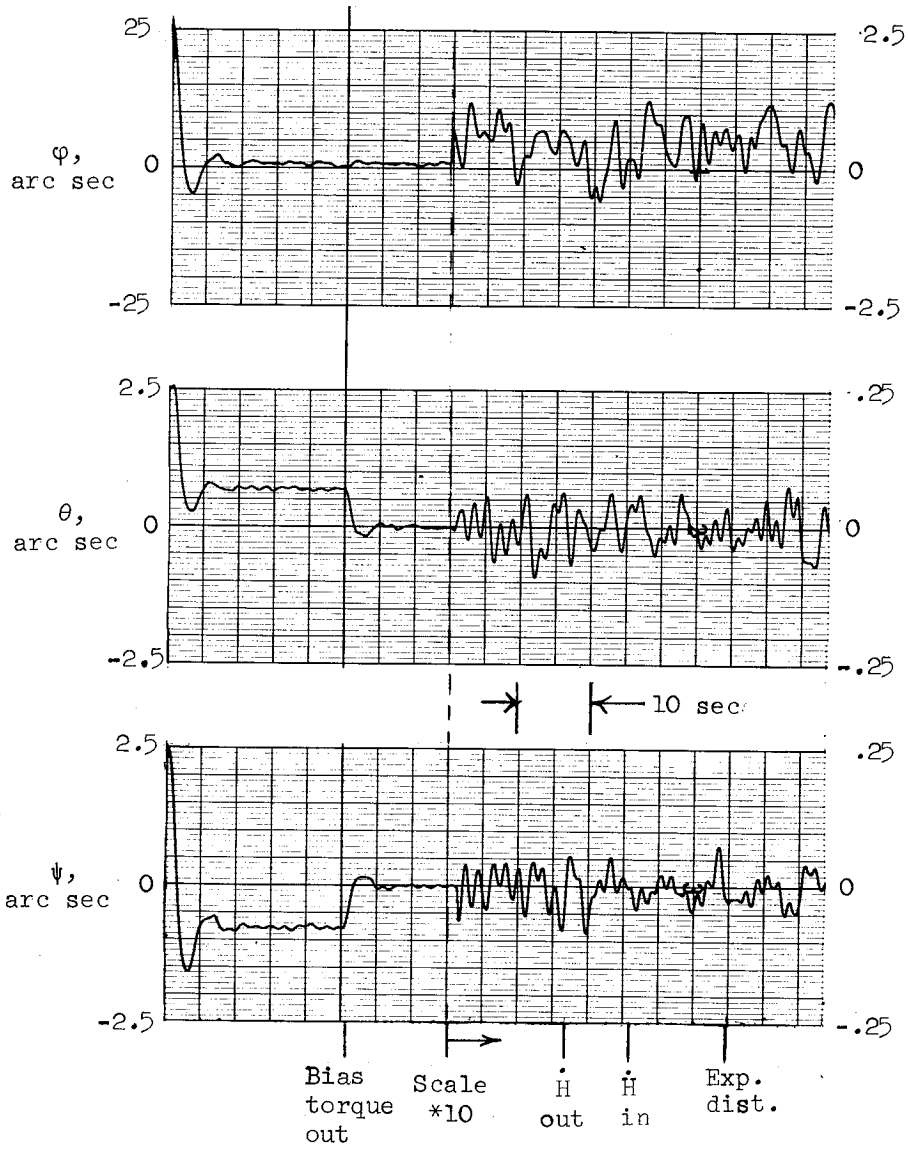

(b) H/2; $\dot{H}$ = 0.2712 N-m per wheel.

Figure 7.- Concluded.

Figure 7 details the fine-pointing capability of IPACS. The two control axes (Y and Z) are subjected to constant bias torques of 1.315 N-m which are the peak magnitude of the combined aerodynamic and gravity-gradient disturbances on the RAM spacecraft. This is taken as the "worst case," even though the two do not usually peak at the same time. The spacecraft offset errors due to the bias torques are approximately 0.7 arc second.

Another question concerning IPACS operation involves the effects of gyro-wheel acceleration and deceleration while adding power to or drawing power from the system.

Figure 7 includes $\dot{H}$ values of 0.2712 N-m per wheel which is the average rate of power consumption during the night cycle. This value is determined from a 50-percent wheel-speed reduction over the 34-minute orbit night. It can be seen that the compensation is effective and that no spacecraft errors result from these torques. The transients produced in switching the $\dot{H}$ on and off are also shown on an expanded scale with the external disturbance bias removed. The transient spacecraft errors are not detectable about the control axes.

The effect of an experiment-induced disturbance (telescope protective door opening) as typified by Skylab data (ref. 7) is also shown in figure 7(a). The experiment-disturbance approximation is shown in the inset of figure 7(a). The resulting spacecraft attitude excursions for both full and half momentum are not discernible. In addition, figure 7 indicates the spacecraft and steady-state motions due to hardware noise and nonlinearities on the expanded scale. The torque feedback loop significantly smooths the error amplitude. Without torque feedback, the excursions peak at about 0.2 arc second for the control axes. The spacecraft angular errors about the two control axes (Y and Z) due to torque measurement are obtained from

$$\theta_{TMS} = \frac{(\text{TMS threshold}) \times 125}{K_{Y,a}} = 0.31 \text{ arc second} \tag{6}$$

This agrees well with the observed value. With the torque feedback loop, maximum amplitudes of approximately 0.05 arc second for full momentum (fig. 7(a)) and almost double that value for the H/2 case (fig. 7(b)) make these motions well within the pointing requirements for the RAM A303B mission, but outside the pointing stability requirements. This is felt to be a result of an interaction between the IPACS unit and TMS, rather than a system effect, since it was not repeated in the simulated system case discussed later. Thus, excellent simulated spacecraft pointing has been achieved by using a set of laboratory-model CMG units as IPACS units without special precision design considerations and with torque-measuring-equipment hardware limitations.

The CMG hardware and torque measurement effects were then eliminated by running identical cases with the simulated IPACS units (fig. 5). These data are shown in figure 8 and can be seen to be essentially identical to the hardware data of figure 7.

The effects of $\dot{H}$ transients are seen to be very slight. Spacecraft errors, due to a 0.2712 N-m (per wheel) $\dot{H}$ transient, are approximately 0.02 arc-second. The $\dot{H}$ transients of -2.712 N-m (per wheel), representing very heavy power draws, produced spacecraft errors of 0.03 arc second, as shown in figure 8(b). Thus, it does not appear that transient power demands will significantly affect IPACS performance during high-accuracy pointing tasks.

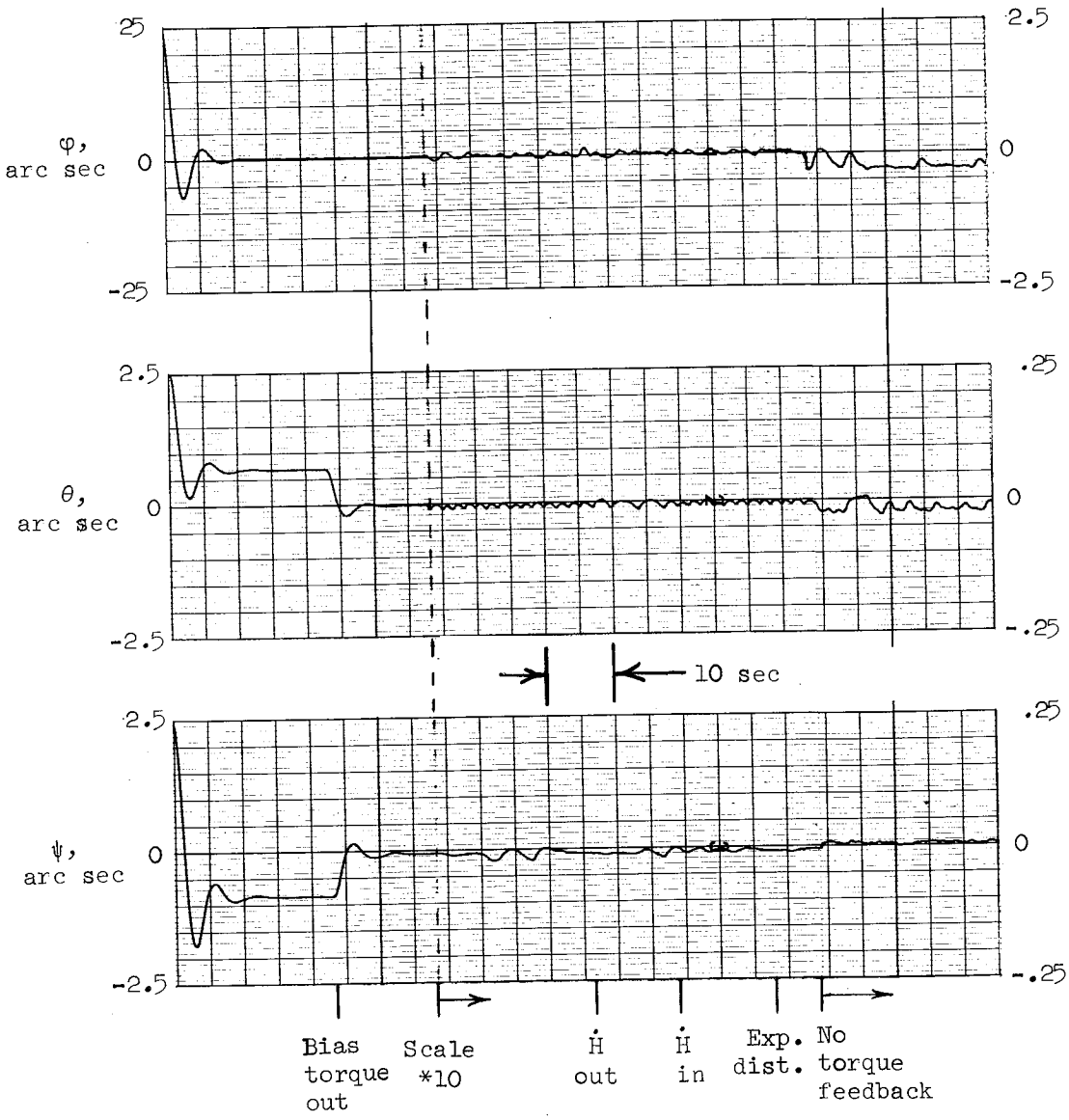

(a) Full H; $\dot{H}$ = -0.2712 N-m per wheel.

Figure 8.- Simulated system response of IPACS.

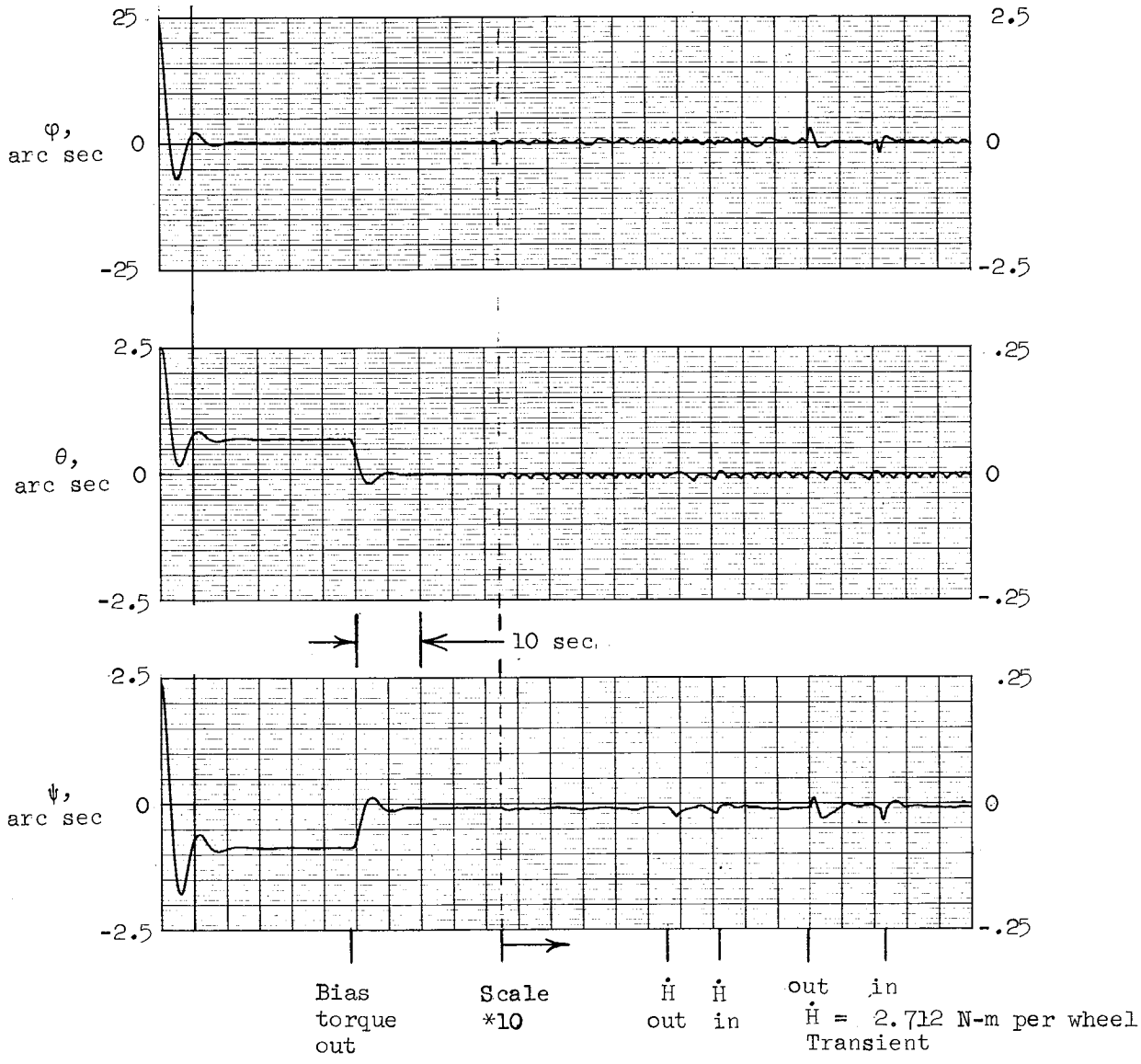

(b) H/2; $\dot{H}$ = 0.2712 N-m per wheel.

Figure 8.- Concluded.

The experiment-induced disturbance (fig. 7(a)) was also applied to the simulated case of figure 8, but it did not drive the spacecraft errors beyond the basic noise amplitude.

It can readily be noted from figure 8 that although the data are essentially identical to the results presented in figure 7, the basic system control threshold is less. This can be attributed to the fact that, with the simulated hardware case, the only remaining limitation on threshold is due primarily to the digital-analog input-output interface. The A/D interface (see fig. 5), transmitting the command moments M_c to

the digital steering law, consists of 12 bits. The command moments are scaled for a maximum value of 203.4 N-m. Thus, the command torque resolution as seen by the digital computer is 0.04963 N-m. Then, for the control (Y and Z) axes, the corresponding angular error threshold is obtained from

$$\theta_{\text{threshold}} = \frac{(M_c)_{\text{threshold}}}{K_{Y,a}} = 0.0245 \text{ arc second} \tag{7}$$

This agrees well with the observed spacecraft errors of about 0.03 arc second for the case with no torque feedback (fig. 8(a)). Again, as in the hardware case, torque feedback improves this situation by reducing the noise error amplitude to approximately 0.015 arc second. It would seem that D/A and A/D scaling for ±14.92 N-m, which is the system maximum torque, would permit 12-bit input-output capability to handle the flight-system interface readily. This was not done in the simulation due to the TMS scaling and to a desire to retain identical scaling of the simulated hardware cases for direct comparison purposes.

CONCLUDING REMARKS

An IPACS concept (Integrated Power and Attitude Control System) has been mechanized with model laboratory prototype CMG (control moment gyroscope) hardware and a digital onboard computer. This system is incorporated in a simulation representing a free-flying RAM (Research and Applications Module) solar mission (A303B) to determine the impact of varying IPACS unit momentum and wheel-acceleration torques associated with power transfer on spacecraft control and pointing capability. A single scissored-pair IPACS unit is considered, which in conjunction with the stringent RAM A303B pointing requirements, represents a "worst case" application of the IPACS concept. The simulation results show that for this condition and with the relatively crude hardware and test equipment used, a high level of pointing can be achieved (1.0 arc second) with perfect sensors. The pointing stability achieved with laboratory hardware (0.05 arc second) did not meet RAM A303B stability requirements. The IPACS concept using simulated IPACS units in place of the hardware was however, readily capable of meeting the stringent solar-mission pointing and stability requirements (1-arc-second pointing accuracy and 0.02-arc-second pointing stability). Control interactions due to power transfer are shown to be minimal, and the resulting spacecraft pointing errors are within mission requirements. This was achieved by calculating the wheel-acceleration torques for use as feedback in the control loop and through the use of a torque feedback scheme. Both of these techniques, however, would represent complications in the onboard control computer calculations.

Overall, the simulation results indicate that the IPACS concept presents no significant problems and is capable of providing the stringent pointing levels required by solar missions. It is also felt that practical IPACS flight hardware could readily be built to meet the pointing stability requirements of 0.02 arc second for the RAM solar astronomy mission.

Langley Research Center,
National Aeronautics and Space Administration,
Hampton, Va., December 14, 1973.

APPENDIX A

SIMULATION EQUATIONS, SCALING, AND DIGITAL COMPUTER ALGORITHMS

Spacecraft Rigid Body

Equations for the spacecraft rigid body, with small-angle approximations, are given as follows:

$$I_X\dot{\omega}_X = G_X$$

$$I_Y\dot{\omega}_Y = G_Y$$

$$I_Z\dot{\omega}_Z = G_Z$$

$$\varphi = \iint \dot{\omega}_X \, dt + \varphi_o$$

$$\theta = \iint \dot{\omega}_Y \, dt + \theta_o$$

$$\psi = \iint \dot{\omega}_Z \, dt + \psi_o$$

where the subscript o denotes initial conditions.

The spacecraft inertias are

$$I_X = 40\ 674 \text{ kg-m}^2$$

$$I_Y = I_Z = 406\ 740 \text{ kg-m}^2$$

where the maximum torques are scaled to be

$$G_X, G_Y, G_Z = \pm 309.7 \text{ N-m}$$

and the spacecraft motions are scaled to be

$$\dot{\omega}_X = \pm 5 \text{ (arc sec)/sec}^2$$

$$\dot{\omega}_Y, \dot{\omega}_Z = \pm 0.5 \text{ (arc sec)/sec}^2$$

$\omega_X = \pm 10$ (arc sec)/sec

$\omega_Y, \omega_Z = \pm 1$ (arc sec)/sec

$\varphi = \pm 100$ arc sec

$\theta, \psi = \pm 10$ arc sec

Spacecraft Control Law

Simple second-order rate plus displacement control law was selected for straightforward response and ease of analysis. The equations for this law are given as follows:

$$M_{X,c} = K_{X,a}\varphi + K_{X,r}\omega_X$$

$$M_{Y,c} = K_{Y,a}\theta + K_{Y,r}\omega_Y$$

$$M_{Z,c} = K_{Z,a}\psi + K_{Z,r}\omega_Z$$

where the gains are

$$K_{i,a} = -I_i\omega_n^2$$

$$K_{i,r} = -2I_i\rho_n\omega_n$$

where

$i = X,\ Y,$ and Z

$\omega_n = 1$ rad/sec

$\rho_n = 0.5$

The maximum command moments are scaled to be

$$M_{i,c} = \pm 203.4 \text{ N-m}$$

Simulated CMG Units

The CMG unit momentum and the gimbal-dynamics equations are given as follows:

$$H = H_o + \int \dot{H}\, dt$$

$$\ddot{\alpha} + 2\rho\omega\dot{\alpha} + \omega^2\alpha = \dot{\alpha}_c$$

where

$$\omega = 15 \text{ rad/sec}$$

$$\rho = 0.4$$

the gimbal motions are scaled to be

$$\dot{\alpha}_c = \pm 6 \text{ deg/sec}$$

$$\dot{\alpha} = \pm 6 \text{ deg/sec}$$

$$\alpha = \pm 200 \text{ deg}$$

Control Torque Calculations

The equations for the torques applied to the spacecraft by the individual CMG units are given as follows:

$$G_{X,j} = H_j\left(\dot{\alpha}_j \cos\alpha_j \cos\beta_j - \dot{\beta}_j \sin\alpha_j \sin\beta_j\right) + \dot{H}_j \sin\alpha_j \cos\beta_j$$

$$G_{Y,j} = -H_j\dot{\beta}_j \cos\beta_j - \dot{H}_j \sin\beta_j$$

$$G_{Z,j} = -H_j\left(\dot{\alpha}_j \sin\alpha_j \cos\beta_j + \dot{\beta}_j \cos\alpha_j \sin\beta_j\right) + \dot{H}_j \cos\alpha_j \cos\beta_j$$

and the total torques are

$$G_X = -G_{X,1} - G_{X,2}$$

$$G_Y = -G_{Y,1} - G_{Y,2}$$

$$G_Z = -G_{Z,1} - G_{Z,2}$$

where j is the CMG number (j = 1,2) and the CMG momentum at full energy storage is given as

$$H_j = 2224 \text{ N-m-sec}$$

The maximum CMG torques are scaled to be

$$G_{X,Y,Z} = \pm 203.4 \text{ N-m}$$

APPENDIX B

FORTRAN LISTING OF CMG SYSTEM STEERING LAW

The following is a FORTRAN listing of the onboard digital routine (subroutine SCPAIR) as programed on the EAI 640. This transformation algorithm represents the steering law for the IPACS scissored-pair CMG configuration. The command moments from the system control law and the CMG gimbal positions are used to calculate command CMG gimbal rates (eqs. (1) to (3)) which will produce the desired command torques. The FORTRAN listing includes comment cards describing the calculations which are given as follows:

```
      SUBROUTINE SCPAIR
C
C     ***     CALCULATE CMG GIMBAL ANGLES FROM SINE-COSINE POTS
        BETA(1)=ATAN2(SB(1),CB(1))
        ALPH(1)=ATAN2(SA(1),CA(1))
        BETA(2)=ATAN2(SB(2),CB(2))
        ALPH(2)=ATAN2(SA(2),CA(2))
C
C     ***     COMPUTE DIRECTION COSINES
        E11=CB(1)*SA(1)
        E13=CB(1)*CA(1)
        E21=CB(2)*SA(2)
        E23=CB(2)*CA(2)
C
C     ***     CALCULATE CONTROL SYSTEM TORQUES DUE TO H-DOTS
        GXHD=HD1*E11+HD2*E21
        GYHD=-HD1*SB(1)-HD2*SB(2)
        GZHD=HD1*E13+HD2*E23
C
C   ***  H-DOT LOGIC TO APPLY AND REMOVE POWER TRANSIENTS
        IF(.NOT. SENSW(1)) GO TO 25
        GXHD=0.
        GYHD=0.
        GZHD=0.
    25  CONTINUE
C
C     ***     CALCULATE CMG SYSTEM MOMENTUM COMPONENTS
        HX1=H1*E11
        HY1=-H1*SB(1)
        HZ1=H1*E13
        HX2=H2*E21
        HY2=-H2*SB(2)
        HZ2=H2*E23
        HX=HX1+HX2
        HY=HY1+HY2
        HZ=HZ1+HZ2
        HT=SQRT(HX*HX+HY*HY+HZ*HZ)
        IF(HT .LT. HTLIM) HT=HTLIM
C
C     ***     LIMIT COMMAND MOMENTS
        AMXC=ABS(MXC)
        AMYC=ABS(MYC)
        AMZC=ABS(MZC)
        IF(AMXC .GT. AL) MXC=SIGN(AL,MXC)
        IF(AMYC .GT. AL) MYC=SIGN(AL,MYC)
        IF(AMZC .GT. AL) MZC=SIGN(AL,MZC)
C
C     ***     CMG SYSTEM STEERING LAW
        IF(BETA(1) .LT. 0.) BETA(1)=BETA(1)+6.28318
        IF(BETA(2) .LT. 0.) BETA(2)=BETA(2)+6.28318
        ALPHA=.5*(ALPH(1)+ALPH(2))
        SINA=SIN(ALPHA)
        COSA=COS(ALPHA)
        DELT=ABS(.5*(BETA(1)-BETA(2)))
        BETAT=.5*(BETA(1)+BETA(2))
        IF(DELT .LT. 1.5708) GO TO 50
        DELT=3.14159-DELT
        BETAT=3.14159+BETAT
    50  SIND=SIN(DELT)
    21  COSB=COS(BETAT)
        SINB=SIN(BETAT)
        BETD=(MXC*SINA*SINB+MYC*COSB+MZC*COSA*SINB)/HT
        DELTD=(MXC*SINA*COSB-MYC*SINB+MZC*COSA*COSB)
        DELTD=.5*DELTD/(H1*SIND)
        RBETA(1)=BETD+DELTD
        RBETA(2)=BETD-DELTD
    60  ALPHD=-(MXC*COSA-MZC*SINA)/(HT*COSB)
        RALPH(1)=ALPHD
C     ****    OUTER GIMBAL NULLING CIRCUIT
        RALPH(2)=ALPHD+GAIN*(ALPH(1)-ALPH(2))
C   ***  SCISSOR ANGLE CUTOFF LOGIC
        IF(ABS(SIND) .LT. GIMLIM .AND. DELTD .LT. 0.) GO TO 61
        GO TO 62
    61  CONTINUE
        RBETA(1)=0.
        RBETA(2)=0.
    62  CONTINUE
        RETURN
        END
```

REFERENCES

1. Kurzhals, Peter R.; and Grantham, Carolyn: A System for Inertial Experiment Pointing and Attitude Control. NASA TR R-247, 1966.

2. Chubb, W. B.; and Seltzer, S. M.: Skylab Attitude and Pointing Control System. NASA TN D-6068, 1971.

3. Lawson, Louis J.: Design and Testing of High Energy Density Flywheels for Application to Flywheel/Heat Engine Hybrid Vehicle Drives. Paper presented at 1971 Intersociety Energy Conversation Engineering Conference (Boston, Mass.), Aug. 1971.

4. Dugger, G. L.; Brandt, A.; George, J. E.; and Penini, L. L.: Flywheel and Flywheel/Heat Engine Hybrid Propulsion Systems for Low-Emission Vehicles. Paper presented at 1971 Intersociety Energy Conversion Engineering Conference (Boston, Mass.), Aug. 1971.

5. Rabenhorst, David W.: Potential Applications for the Superflywheel. Paper presented at 1971 Intersociety Energy Conversion Engineering Conference (Boston, Mass.), Aug. 1971.

6. Kennedy, H. B.: A Gyro Momentum Exchange Device for Space Vehicle Attitude Control. AIAA J., vol. 1, no. 5, May 1963, pp. 1110-1118.

7. Anon.: Research and Applications Modules (RAM) Phase B Study – Preliminary Technical Data Document. Vol. II, Appendix A, Pt. IX. Rep. No. GSCA-DDA71-004 (Contract NAS 8-27539), General Dynamics, Dec. 17, 1971. (Available as NASA CR-123785.)

NASA-Langley, 1974 L-8791